Journal of Low Temperature Physics
https://doi.org/10.1007/s10909-023-03038-1

Thermalization of a SQUID Chip at Cryogenic Temperature: Thermal Conductance Measurement for GE 7031 Varnish Glue, Apiezon N Grease and Rubber Cement Between 20 and 200 mK

M. D'Andrea[1] · G. Torrioli[2] · C. Macculi[1] · M. Kiviranta[3]

Received: 2 November 2023 / Accepted: 30 December 2023

Abstract
In the context of the ATHENA X-IFU Cryogenic AntiCoincidence detector (CryoAC) development, we have studied the thermalization properties of a 2×2 mm SQUID chip. The chip is glued on a front-end PCB and operated on the cold stage of a dilution refrigerator ($T_{\mathrm{BASE}}<20$ mK). We performed thermal conductance measurements by using different materials to glue the SQUID chip on the PCB. These have been repeated in subsequent cryostat runs, to highlight degradation effects due to thermal cycles. Here, we present the results obtained by glues and greases widely used in cryogenic environments, i.e., GE 7031 Varnish Glue, Apiezon N Grease and Rubber Cement.

Keywords ATHENA · CryoAC · SQUID thermalization · Cryogenic glues · Thermal conductance

1 Introduction

We are developing the Cryogenic AntiCoincidence detector (CryoAC [1, 2]) of the ATHENA X-ray observatory [3]. It is a particle detector aimed to reduce the background of the X-IFU, the on-board X-ray spectrometer [4]. The CryoAC is a 4-pixel silicon detector, sensed by transition edge sensors (TES) and readout by four independent single-stage SQUIDs operated in flux-locked-loop (FLL) mode. The SQUID chips are glued on the detector CFEE PCB (cold front-end electronics

✉ M. D'Andrea
matteo.dandrea@inaf.it

[1] INAF/IAPS, Via del Fosso del Cavaliere 100, 00133 Rome, Italy

[2] CNR/IFN Roma, Via del Fosso del Cavaliere 100, 00133 Rome, Italy

[3] VTT, Tietotie 3, 02150 Espoo, Finland

Published online: 25 January 2024

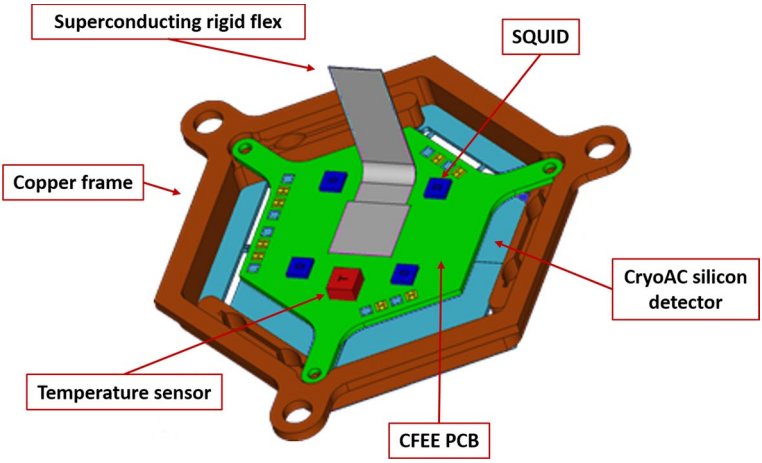

Fig. 1 The Cryogenic Anticoincidence detector (CryoAC) cold stage (50 mK) assembly concept. (Color figure online)

printed circuit board) located in the cold stage, at $T = 50$ mK. The CryoAC assembly concept is shown in Fig. 1.

The selection of the glue to be used on the PCB is an ongoing task managed at X-IFU system level, and it is driven by several constraints such as thermal properties, mechanical behavior and chemical composition. The proper glues qualification will be carried out inside the next CryoAC industrial contract (around 2025), and it will follow the standards for space product assurance (see [5] for detail about adhesive bonding qualification for space applications).

In this context, we have preliminarily investigated the thermal properties of different glues and greases widely use in cryogenic environments, in order to have a first reference for the CryoAC development activity.

2 Experimental Setup

We have directly studied the thermalization of a SQUID chip glued on a CFEE PCB prototype featuring superconducting Al traces (designed by us and provided by Omni Circuit Boards[1]). The system has been anchored on the cold stage of a dilution refrigerator, with a base temperature $T_{\mathrm{BASE}} < 20$ mK.

The SQUID chip features two very low-ohmic embedded resistors, usually used to shunt the CryoAC TES. We connected one of these to the SQUID input coil, to use the device as a Johnson noise thermometer. By varying the SQUID working point, we measured the actual chip temperature for different power loads (due to the SQUID bias) and different cold stage temperatures, effectively measuring

[1] https://www.omnicircuitboards.com/

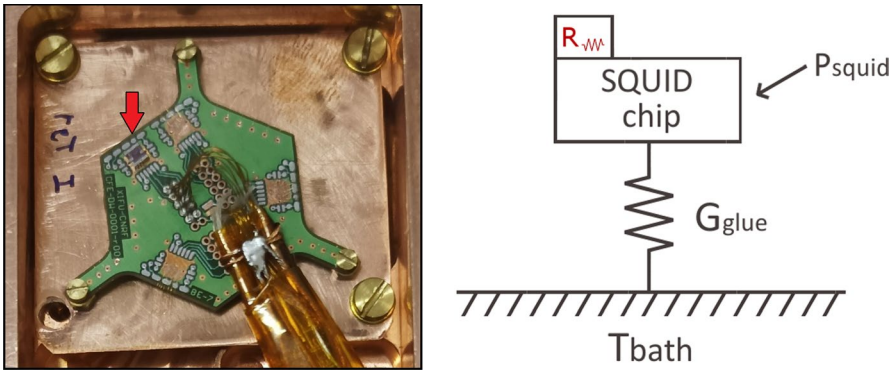

Fig. 2 *Left* Picture of the experimental setup, showing the SQUID chip (red arrow) glued on the CFEE PCB prototype. *Right* Thermal model of the system. The resistor "*R*" is embedded on the SQUID chip. P_{SQUID} is given by the SQUID bias, and T_{bath} is the temperature of PCB copper ground plane, strongly anchored to the cryostat cold stage. G_{glue} is the thermal conductance of the glue used to bond the SQUID chip to the PCB. (Color figure online)

the thermal conductance between the chip and the thermal bath. The latter is represented by the PCB copper ground plane, which has been strongly coupled to the mixing chamber via screws and gold bonding wires.

We have performed the measurements by using different materials to glue the SQUID on the PCB, i.e., GE 7031 Varnish Glue,[2] Apiezon N Grease[3] and Rubber Cement.[4] Furthermore, for each material, we have repeated the measurements in two subsequent cryostat runs, to highlight degradation effect due to thermal cycle.

A picture and a thermal schematic of the setup are shown in Fig. 2.

2.1 SQUID schematics and characteristics

The SQUID used for the measurements is a series array model M4A produced by VTT [6]. It has been deposited on a 2 mm × 2 mm silicon chip (675 μm thick), where only the top surface has been polished. Its schematics, both in term of circuitry and pads layout, are shown in Fig. 3.

In addition to the standard circuitry for SQUID operations (i.e., input and feedback coils), the chip features two very low-ohmic resistors, with $R_1 = 0.5$ mΩ and $R_2 = 2.2$ mΩ nominal values. Here, the 0.5-mΩ resistor has been directly connected to the input coil via aluminum bonding wires, to use the device as Johnson noise thermometer (red connections in Fig. 3 *Left*). The chip features are also an embedded heater, which has not been used for this application.

[2] Commercialized as "IMI 7031 insulating varnish" from GVL Cryoengineering, http://www.gvl-cryoengineering.de/

[3] https://apiezon.com/products/vacuum-greases/apiezon-n-grease/

[4] Commercialized as "PAX Rubber Cement (Solution)", https://pax.com.tw/

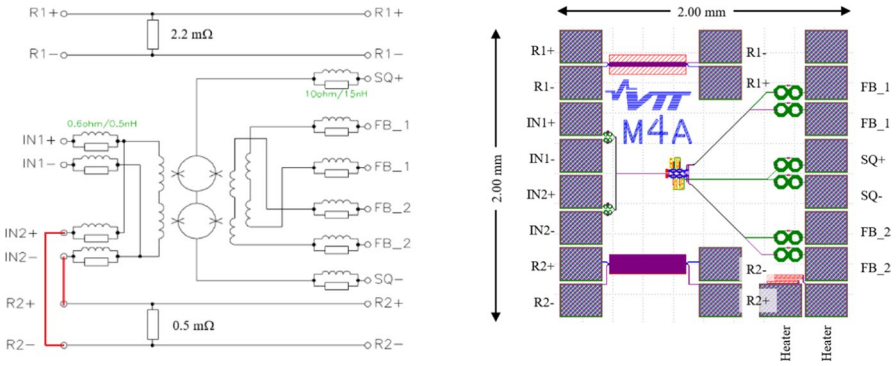

Fig. 3 VTT SQUID series array M4A schematics. *Left* Simplified internal schematics. For these measurements, the R2 resistor has been directly connected to the SQUID input coil (red lines). *Right* Pad layout and chip size. (Color figure online)

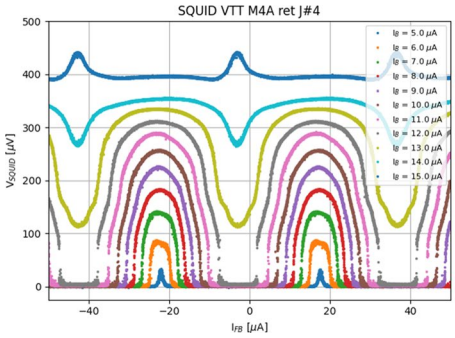

Parameter	Value
$1/M_{IN}$	12.1 μA/Φ$_0$
$1/M_{FB1}$	36.7 μA/Φ$_0$
$1/M_{FB2}$	39.7 μA/Φ$_0$
R_1	(2.14 ± 0.02) mΩ
R_2	(0.51 ± 0.01) mΩ

Fig. 4 Left Characteristics V–Φ curves of the SQUID acquired at 50 mK through the feedback line, for different bias currents. Right Measured values of the main SQUID parameters. $1/M_{IN}$, $1/M_{FB1}$ and $1/M_{FB2}$ are the input and feedbacks mutual inductance, and R_1 and R_2 are the embedded resistors. (Color figure online)

The SQUID has been operated by a commercial Magnicon XXF-1 electronics.[5] The characteristics V–Φ curves and the measured value of its main parameters are shown in Fig. 4. Around the maximum gain working point ($I_B \sim 12.0$ μA, $V_{SQUID} \sim 200$ μV, $dV/d\Phi \sim 3$ mV/Φ$_0$), the SQUID has a typical power dissipation $P_{SQUID} \sim 2.4$ nW.

[5] http://www.magnicon.com/squid-electronics/xxf-1

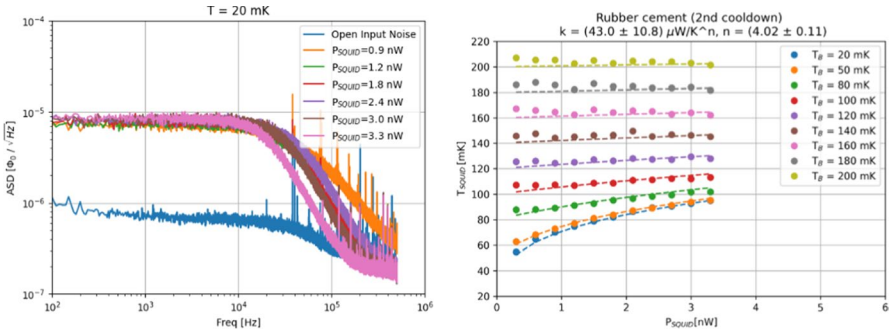

Fig. 5 *Left* Noise spectra acquired at a fixed bath temperature ($T_B = 20$ mK), used to evaluate the chip temperature as a function of the power load. The blue curve represents the total system noise at open input, previously measured. (Color figure online). *Right* Thermal conductance measurement. The SQUID chip temperature (evaluated from Johnson noise) is reported as function of power load, for different bath temperatures. Data have been fitted with Eq. (3) (dashed lines). (Color figure online)

3 Thermal Conductance Measurements

To measure the thermal conductance between SQUID and PCB (G_{GLUE}), we monitored the chip temperature (T_{SQUID}) for different power loads (P_{SQUID}) and thermal bath temperatures (T_B).

The power loads on the SQUID are set by its bias point, and it has been evaluated from the acquired characteristic curves (for each bias point, $P_{\mathrm{SQUID}} = I_{\mathrm{B}} \cdot V_{\mathrm{SQUID}}$). The chip temperature has been evaluated by measuring the white noise at the SQUID output (W_{n} [$\Phi_0/\sqrt{\mathrm{Hz}}$]), which is due to the Johnson noise of the resistor connected to the input coil (I_{n} [$A/\sqrt{\mathrm{Hz}}$]) [7]:

$$W_{\mathrm{n}} = \frac{1}{M_{\mathrm{IN}}} \cdot I_{\mathrm{n}} = \frac{1}{M_{\mathrm{IN}}} \sqrt{\left(4 \cdot k_B \cdot T_{\mathrm{SQUID}}\right)/R_2} \tag{1}$$

$$T_{\mathrm{SQUID}} = \left(W_{\mathrm{n}} \cdot \frac{1}{M_{\mathrm{IN}}}\right)^2 \cdot \frac{R_2}{4 \cdot k_{\mathrm{B}}} \tag{2}$$

where $1/M_{\mathrm{IN}}$ is the input coil coupling, $R_2 = 0.5$ mΩ and k_{B} is the Boltzmann constant. Figure 5 *Left* shows the noise spectra acquired at a fixed bath temperature for different SQUID power loads (i.e., different SQUID bias point). W_n has been evaluated as the average noise value in the 200 Hz–3 kHz frequency range. Note that the typical total system noise at open input (blue line in Fig. 5 *Left),* mainly due to the electronics pre-amplifier and previously measured, is negligible with respect to the Johnson noise. Therefore, we are confident that the measured noise is given by the R_2 Johnson component.

To evaluate the glue thermal conductance, the acquired data have been finally fitted with the standard power-law model describing the power flow to the heat bath [8]:

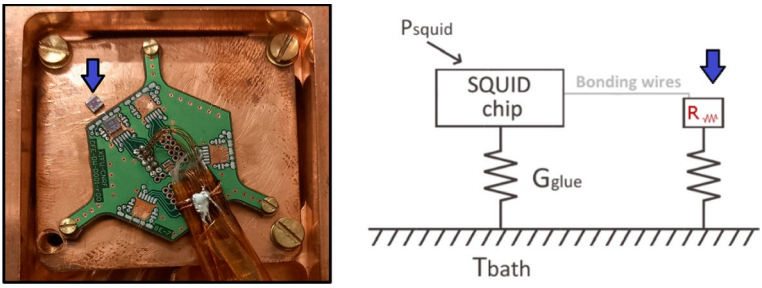

Fig. 6 *Left* Picture of the control measurement setup. A second chip (blue arrow) is glued directly to the thermal bath. Its embedded resistor is connected to the PCB SQUID via Al bonding wires, to perform Johnson noise thermometry. *Right* Thermal model of the control setup. Note that the second chip (blue arrow) has not direct power loads. (Color figure online)

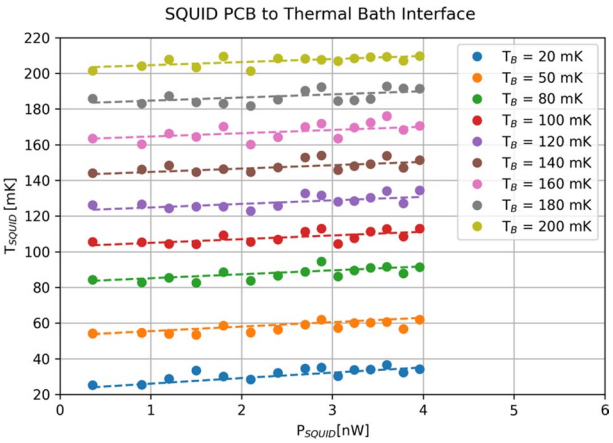

Fig. 7 Results of the control measurements. The temperature of the second chip is monitored as a function of the PCB SQUID power, for different thermal bath temperatures. (Color figure online)

$$P_{\mathrm{SQUID}} = k \cdot \left(T^{n}_{\mathrm{SQUID}} - T^{n}_{B} \right) \tag{3}$$

where k and n are the fit parameters, related the nature of the thermal link. The final measured thermal conductance is as follows:

$$G_{\mathrm{GLUE}}(T) = n \cdot k \cdot T^{(n-1)} \tag{4}$$

One of the performed measurements is presented in Fig. 5 *Right (*see the Appendix 1 for the complete set of measurements). Note that, due to the non-ideal thermal coupling between the SQUID chip and the PCB (which is strongly anchored to the bath), at low temperature, the chip is significantly warmer than the bath temperature.

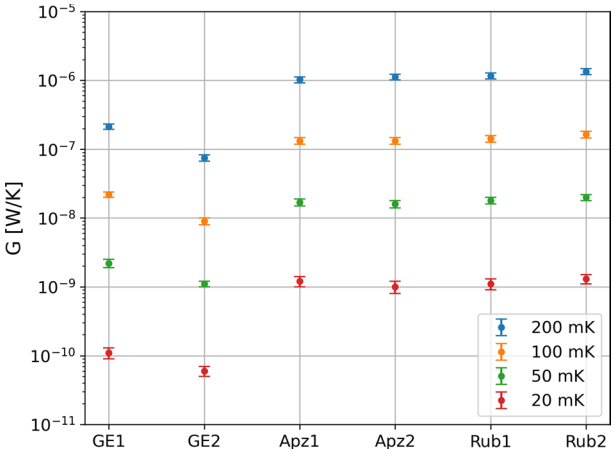

Fig. 8 Summary of the thermal conductance measurements performed with different materials (GE-7031 Varnish Glue, Apiezon N Grease and Rubber Cement) in subsequent thermal cycles. (Color figure online)

3.1 Control Measurement

We performed also a control measurement to check potential systematic setup effects. In this case, we measured the temperature of a second SQUID chip (with embedded resistor) directly glued to the copper plate hosting the PCB, i.e., to the thermal bath. Also here, we performed Johnson noise thermometry by connecting only the resistor of the second chip to the PCB SQUID input coil (via aluminum bonding wires). A picture and a thermal schematic of the control setup are shown in Fig. 6.

The result of the control measurement is reported in Fig. 7. In this case, we found a good thermalization of the chip, with its temperature always close to the thermal bath one, especially at low-power values. This is expected, since in this configuration, the monitored chip has not direct power loads. The slight dependence of the chip temperature from the PCB SQUID power is probably due to parasitic heat load, mainly due to the aluminum bonding wires.

This measurement shows that no significant systematic effect affects the setup, and that it is possible perform a proper Johnson noise thermometry down to ~20–30 mK by this setup. This is important to exclude, for example, possible effects due to the electron–phonon decoupling in the monitored resistor. The electron–phonon conductance has indeed a strong dependence from the temperature, with thermal power index $n \sim 5$–6 [8, 9]; thus, it could be a limiting factor for measurements at ultra-low temperature.

Furthermore, the measurements guarantees that all the additional component in the noise (i.e., SQUID, pre-amplifier and DAQ noise) are effectively negligible with respect to the Johnson noise of the resistor.

Table 1 Summary of the thermal conductance measurements performed with different materials and in subsequent thermal cycles

Dataset	k [μW/K]	n	G @ 50 mK [nW/K]	G @ 100 mK [nW/K]
GE-7031 (1st cooldown)	10.2 ± 1.1	4.30 ± 0.06	2.2 ± 0.3	22 ± 2
GE-7031 (2nd cooldown)	2.7 ± 0.2	4.09 ± 0.04	1.1 ± 0.1	9 ± 1
Apiezon N (1st cooldown)	29.9 ± 6.8	3.95 ± 0.10	17 ± 2	133 ± 15
Apiezon N (2nd cooldown)	38.5 ± 7.7	4.07 ± 0.09	16 ± 2	133 ± 15
Rubber Cement (1st cooldown)	37.3 ± 7.8	4.02 ± 0.09	18 ± 2	143 ± 16
Rubber Cement (2nd cooldown)	43.0 ± 10.8	4.02 ± 0.11	20 ± 2	165 ± 18

4 Results

The results of the measurements performed with the different glues are summarized in Fig. 8 and Table 1. For each material, they are reported the best-fit k and n parameters and the resulting thermal conductance (evaluated at different temperatures) in two subsequent cooldowns.

The gluing of the SQUID chip has been always performed by hand, in air, without any curing procedure. The bond line thickness was of the order of 50 μm, roughly controlled by visual inspection. Air bubbles were removed from the bonding agents before placing the chip on the PCB. In each cryostat run, the setup undergo a vacuum pump-down (from 1000 mbar to $< 10^{-4}$ mbar) and a full thermal cycle from 300 K to 20 mK.

We observe that GE 7031 shows the worst thermal conductance at cold and a significant degradation with thermal cycle. Rubber Cement and Apiezon N grease show similar thermal properties, without significant degradation in the 2nd cooldown and with G of the order of 150 nW/K @100 mK.

Note that the best-fit power index n is always compatible with the value $n = 4$, as expected for a Kapitza (i.e., boundary) interface [9].

5 Conclusions

In the context of the ATHENA X-IFU Cryogenic AntiCoincidence detector (CryoAC) development, we have studied the thermalization properties of a 2×2 mm SQUID chip bonded on a PCB with different gluing materials. Table 1 and Fig. 8 are reported the measured thermal conductance for GE-7031 Varnish Glue, Apiezon N Grease and Rubber Cement between 20 and 200 mK, in two subsequent thermal cycles. These values represent a first reference for the CryoAC development activity and worth of notice for the whole low-temperature detector community.

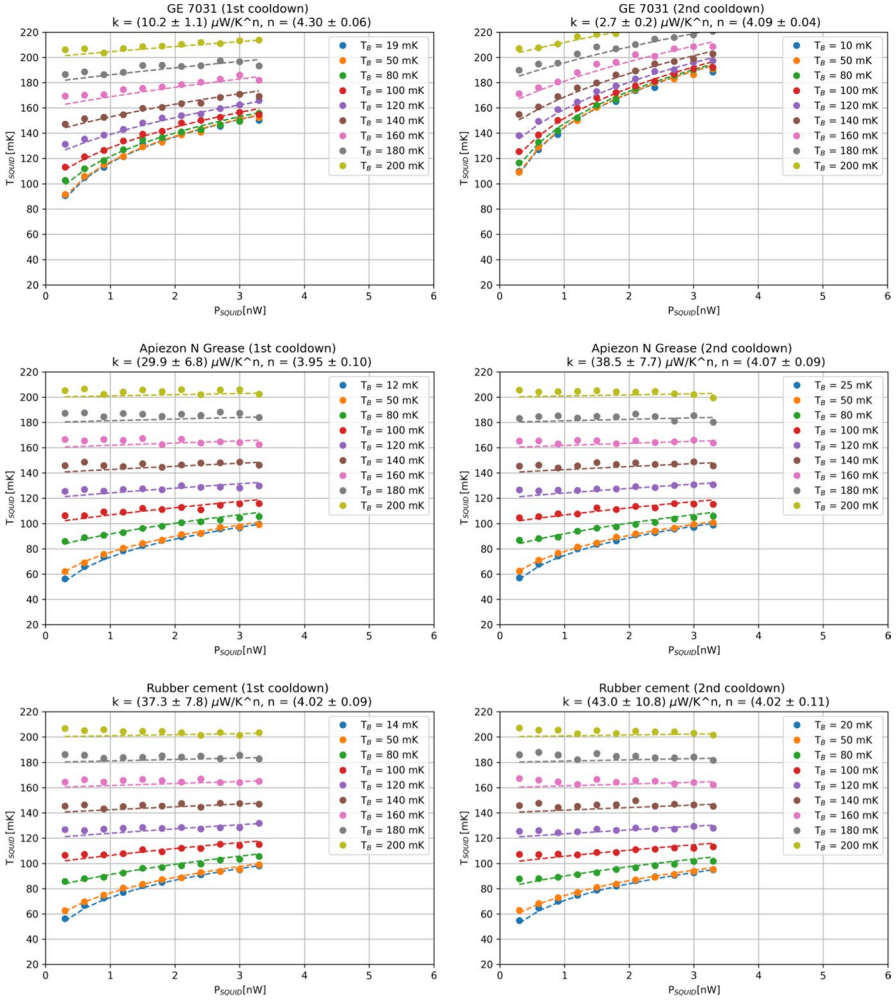

Fig. 9 Thermal conductance measurements (T_{SQUID} vs. P_{SQUID} for different thermal bath temperatures) performed for different gluing materials (*Top* GE 7031, *Middle* Apiezon N Grease and *Bottom* Rubber Cement) in two subsequent cryostat runs (*Left* 1st cooldown and *Right* 2nd cooldown). Setup as from Fig. 2. (Color figure online)

Finally, we report that the next-generation CryoAC SQUIDs, currently under development at VTT, will include also a gold bonding pad. This will allow, if needed, to further improve the SQUID chip thermalization via gold bonding wires.

Appendix 1

The full set of thermal conductance measurements performed is reported in Fig. 9.

Acknowledgements This work has been supported by ASI (Italian Space Agency) contract n. 2019-27-HH.0. The authors would like to thank Jan van der Kuur (SRON) for useful discussion. M.D. thanks Ciclofisica (the Ciclofficina «Roberto Perciballi») for the Rubber Cement supply.

Author contributions MD, GT, CM conceived and planned the experiment, prepared the experimental setup and performed the measurements. MK designed and produced the SQUID. MD performed data analysis and all authors discussed the results. MD wrote the manuscript with inputs from all authors.

Funding Open access funding provided by Istituto Nazionale di Astrofisica within the CRUI-CARE Agreement.

Declarations

Conflict of interest The authors declare no competing interests.

References

1. C. Macculi et al., The cryogenic Anticoincidence detector for the newAthena X-IFU instrument: a program overview. Condens. Matter **8**, 108 (2023). https://doi.org/10.3390/condmat8040108
2. M. D'Andrea et al., The TES-based cryogenic anticoincidence detector (CryoAC) of ATHENA X-IFU: a large area silicon microcalorimeter for background particles detection. J. Low Temp. Phys. (2023). https://doi.org/10.1007/s10909-023-03034-5
3. X. Barcons et al., Athena: ESA's X-ray observatory for the late 2020s. Astron. Nachr AN **338**, 153–158 (2017). https://doi.org/10.1002/asna.201713323
4. D. Barret et al., The athena X-ray integral field unit: a consolidated design for the system requirement review of the preliminary definition phase. ExpA **55**, 373–426 (2023). https://doi.org/10.1007/s10686-022-09880-7
5. ECSS Secretariat, ECSS-Q-ST-70-16C: Adhesive bonding for spacecraft and launcher applications (1 December 2020), https://ecss.nl/standard/ecss-q-st-70-16c-adhesive-bonding-for-spacecraft-and-launcher-applications-1-december-2020/
6. M. Kiviranta et al., Two-stage SQUID amplifier for the frequency multiplexed readout of the X-IFU X-ray camera. IEEE-TAS **31**(5), 1–5 (2021). https://doi.org/10.1109/TASC.2021.3060356
7. F. Pobell, *"Low-temperature thermometry", in matter and methods at low temperatures* (Springer, Berlin, 2007)
8. K. Irwin, G. Hilton, "Transition-edge sensors", in cryogenic particle detection. Top. Appl. Phys. **99**(63), 150 (2005)
9. M. D'Andrea (2019) Opening the low-background and high-spectral-resolution domain with the ATHENA large X-ray observatory: development of the cryogenic anticoincidence detector for the X-ray integral field unit, PhD Thesis. https://arxiv.org/pdf/1904.03307.pdf